



Contents lists available at ScienceDirect

# Bioorganic & Medicinal Chemistry Letters

journal homepage: [www.elsevier.com/locate/bmcl](http://www.elsevier.com/locate/bmcl)

## Impact of aryloxy-linked quinazolines: A novel series of selective VEGFR-2 receptor tyrosine kinase inhibitors

Antonio Garofalo<sup>a,b</sup>, Laurence Goossens<sup>a,b,\*</sup>, Perrine Six<sup>a,b</sup>, Amélie Lemoine<sup>a,b</sup>, Séverine Ravez<sup>a,b</sup>, Amaury Farce<sup>a,c</sup>, Patrick Depreux<sup>a,b</sup>

<sup>a</sup> Univ Lille Nord de France, F-59000 Lille, France

<sup>b</sup> UDSL, ICPAL, EA 4481, F-59006 Lille, France

<sup>c</sup> UDSL, UFR de Pharmacie, EA 4481, Laboratoire de Chimie Thérapeutique, F-59006 Lille, France

### ARTICLE INFO

#### Article history:

Received 17 December 2010

Revised 28 January 2011

Accepted 29 January 2011

Available online 3 February 2011

#### Keywords:

Quinazoline

EGFR

VEGFR2

RTK inhibitors

Anticancer agents

### ABSTRACT

Three series of 6,7-dimethoxyquinazoline derivatives substituted in the 4-position by aniline, *N*-methylaniline and aryloxy entities, targeting EGFR and VEGFR-2 tyrosine kinases, were designed and synthesized. Pharmacological activities of these compounds have been evaluated for their enzymatic inhibition of VEGFR-2 and EGFR and for their antiproliferative activities on various cancer cell lines. We have studied the impact of the variation in the 4-position substitution of the quinazoline core. Substitution by aryloxy groups led to new compounds which are selective inhibitors of VEGFR-2 enzyme with IC<sub>50</sub> values in the nanomolar range in vitro.

© 2011 Elsevier Ltd. All rights reserved.

Receptor tyrosine kinases (RTKs) play crucial roles in signal transduction pathways and cellular processes (proliferation, cell cycle, cell metabolism, survival, apoptosis, DNA damage/repair, ...).<sup>1,2</sup> Most signal transduction pathways are mediated by protein kinases, and aberrant kinase signaling leads to proliferation of cancer cells and also angiogenesis and growth of solid tumors such as prostatic, colon, breast, and gastric cancers.<sup>3–5</sup> Vascular endothelial growth factor (VEGF) and receptor protein-tyrosine kinases are the key regulators of angiogenesis, vasculogenesis, and developmental hematopoiesis.<sup>6–8</sup> VEGF is a mitogen and a survival factor for vascular endothelial cells. The VEGF family of receptors consists of three protein-tyrosine kinase receptors (VEGFR-1, VEGFR-2, and VEGFR-3) and two non-protein kinase co-receptors (neuropilin-1 and neuropilin-2). These components participate in new blood vessel formation from angioblasts (vasculogenesis) and new blood vessel formation from pre-existing vasculature (angiogenesis). Interaction between VEGFR-1 and VEGFR-2 or VEGFR-2 and VEGFR-3 alters receptor tyrosine phosphorylation.<sup>9–11</sup> The VEGF receptor protein-tyrosine kinases consist of an extracellular component containing seven immunoglobulin-like domains, a single transmembrane segment, a juxtamembrane segment, and

an intracellular protein-tyrosine kinase domain. VEGFR-2 (Flk-1 mouse, KDR human) is the predominant mediator of VEGF-stimulated endothelial cell migration, proliferation, survival, and enhanced vascular permeability. Although VEGFR-2 has lower affinity for VEGF than VEGFR-1, VEGFR-2 exhibits robust protein-tyrosine kinase activity in response to its ligands. VEGFR-2 is expressed at abnormally high levels in a large variety of human solid tumors.<sup>12,13</sup> Several researchers have been pursuing VEGFR-2 kinase domain inhibitors to discover novel anti-angiogenic drugs. The growing interest in this strategy for cancer treatment stems from the envisioned favorable toxicity profile. Because VEGFR-2 is located essentially in endothelial cells and expressed by several cancer cells, an angiogenesis inhibitor is not expected to affect proliferation of normal cells, unlike conventional cytotoxic chemotherapy. Several successful strategies for the inhibition of angiogenesis have been effectively demonstrated in preclinical and clinical settings, as exemplified by the recent USFDA approval of a humanized anti-VEGF monoclonal antibody (bevacizumab, Avastin®) as a first-line treatment of metastatic colorectal cancer, in combination with chemotherapy.<sup>14,15</sup> Small molecule inhibitors of VEGF receptor protein tyrosine kinases represent another approach for inhibiting angiogenesis. The drug sorafenib (Nexavar®), from Bayer, has recently been approved by the USFDA for the treatment of metastatic renal cell carcinomas.

Quinazoline derivatives have attracted interest over the years because of their multiple biological activities, notably as kinase

\* Corresponding author. Address: Institut de Chimie Pharmaceutique Albert Lespagnol, Univ Lille Nord de France, 3 rue du Professeur Laguesse, B.P.83 59006 Lille, France. Tel.: +33 (0) 3 20 96 47 02; fax: +33 (0) 3 20 96 49 06.

E-mail address: [laurence.goossens@univ-lille2.fr](mailto:laurence.goossens@univ-lille2.fr) (L. Goossens).

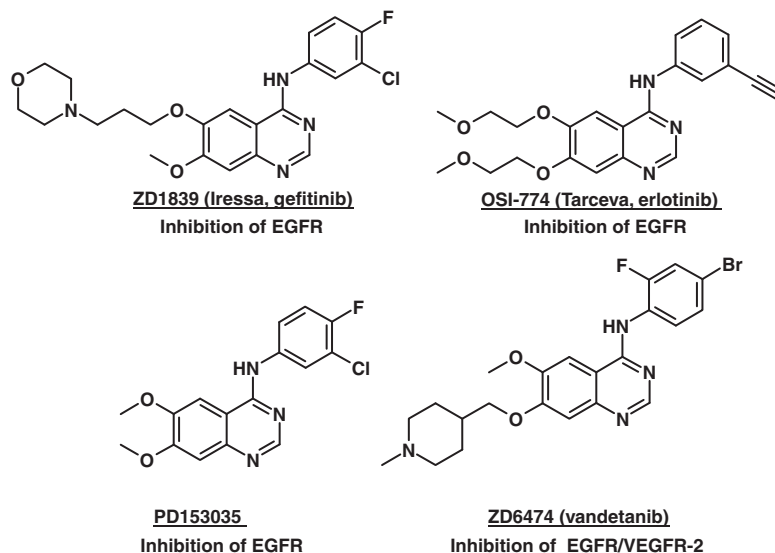


**Figure 1.** Structure of ATP-mimic inhibitors for treatment in solid tumors.

inhibitors.<sup>16,17</sup> The first generation of quinazoline as PD153035 exhibits a high affinity for EGFR but a poor *in vivo* activity.<sup>18,19</sup> The clinical success of selective kinase inhibitors, such as gefitinib (Iressa<sup>®</sup>) and erlotinib (Tarceva<sup>®</sup>), as therapeutic agents for several human cancers has prompted substantial interest in the further development and clinical testing of such inhibitors for a wide variety of malignancies. Vandetanib (ZD6474), from AstraZeneca, a once-daily oral anticancer drug in phase III, is considered to be a dual tyrosine kinase inhibitors targeting EGFR and VEGFR-2 (Fig. 1).<sup>20–25</sup> This quinazoline substituted with a halide at the 2- and 4-positions on the phenyl group shows a strong inhibitory activity ( $IC_{50}$  = 500 nM for EGFR and 40 nM for VEGFR-2, in ELISAs with recombinant enzymes).<sup>26</sup>

The 4-anilinoquinazoline scaffold has to be able to selectively inhibit the tyrosine kinase activity of the epidermal growth factor receptor (EGFR) and also to inhibit simultaneously the tyrosine kinase activity of EGFR and VEGFR. But, to date, no selective inhibition towards VEGFR tyrosine kinase activity was obtained with the 4-anilinoquinazolines. However, an indole-ether quinazoline, AZD2171, is a highly potent ATP-competitive inhibitor of recombinant KDR tyrosine kinase *in vitro*.<sup>27</sup>

These compounds have been designed in view of the known interactions between 4-anilinoquinazolines and the adenine-binding region of the ATP-binding site of these receptors and they have shown a good cytotoxicity against several types of tumors *in vitro*.

We recently described the structure–activity relationships (SAR) developed around anilinoquinazoline derivatives, exemplified by the pharmacophore **1**, as potent EGFR/VEGFR-2 dual kinase inhibitors (Fig. 2).<sup>25,28</sup>

With the aim of further exploring one of the key recognition elements of the kinase inhibitors, which are presumed to bind into

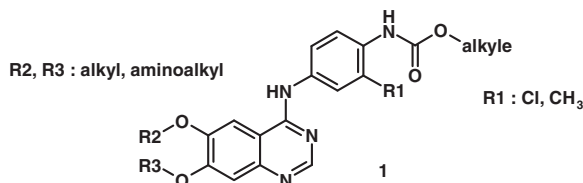
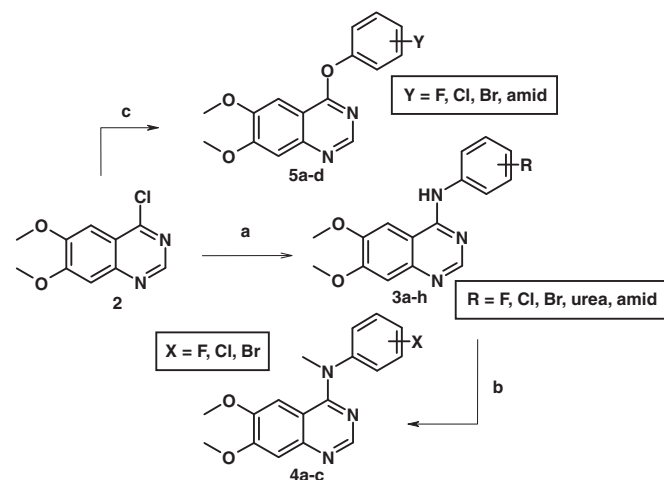
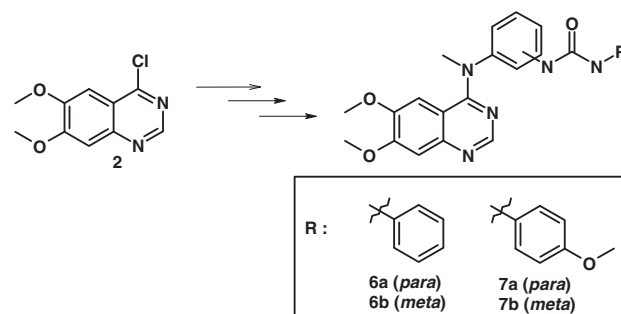


**Figure 2.** Pharmacophore **1** of anilinoquinazoline derivatives, potent dual kinase inhibitor.<sup>25,28</sup>

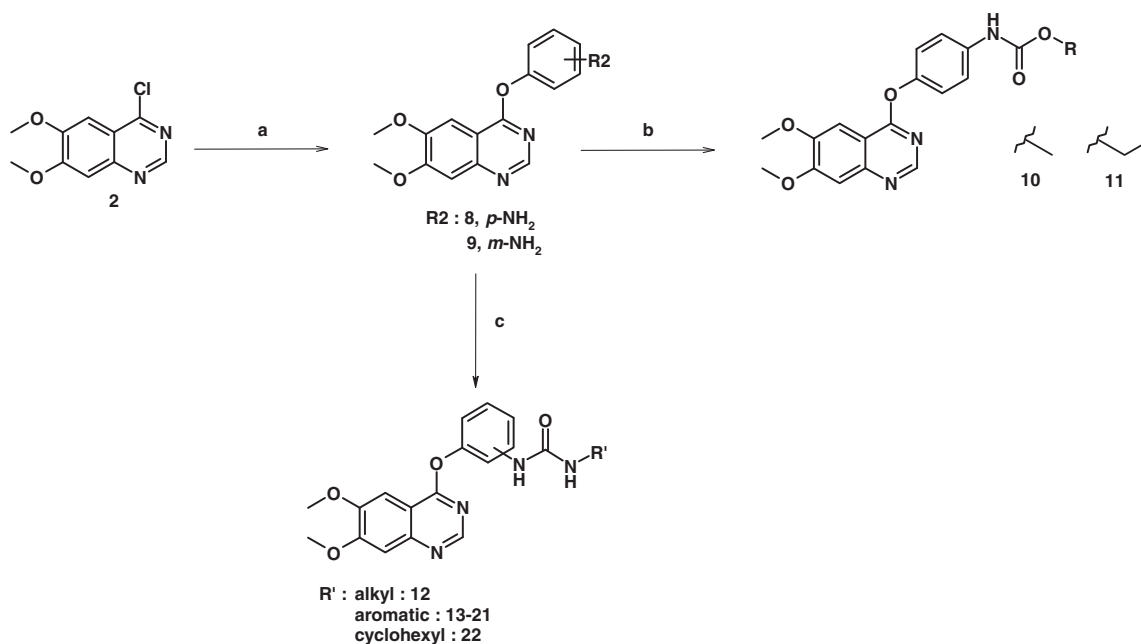
the hydrophobic back pocket of the kinase active site, we envisioned the replacement of the aniline moiety by an *N*-methyl analog and aryloxy groups. According to the X-ray structural analysis,



**Scheme 1.** Reagents and conditions: (a) aniline derivatives, (CH<sub>3</sub>)<sub>2</sub>CHOH, reflux, 80–95%; (b) CH<sub>3</sub>I, NaH, DMF, room temperature, 25–40%; (c) phenol derivatives, NaH, DMSO, 150 °C, 100 W, microwave, 59–65%.



**Scheme 2.** Chemical structure of ureas **6–7**.<sup>19</sup>



**Scheme 3.** Reagents and conditions: (a)  $n\text{Bu}_4\text{N}^+\text{Br}^-$ , 2-butanone, 20% NaOH, reflux, 80% for **8** and 93% for **9**; (b)  $\text{ROCOCl}$ ,  $\text{NEt}_3$ , THF, room temperature, 50–60%; (c) isocyanate derivatives,  $\text{NEt}_3$ ,  $\text{CHCl}_3$ , room temperature, 25–60%.

the NH entity of anilinoquinazoline derivatives does not establish interactions with EGFR or VEGFR-2 enzymatic active-site. Our effort to develop small molecular, ATP-competitive dual EGFR/VEGFR-2 inhibitors led to the development of three series of compounds with different hydrogen bond donor and/or acceptor groups at the 4-position on the quinazoline. We describe here the chemistry, SAR, and biological testing for these series. The quinazoline core was modified at position 4 of the aryl with different bulky substituents such as amide, carbamate or urea, which are commonly-used moieties in EGFR and VEGFR inhibitors with the aim of strengthening the ligand–receptor interactions and therefore increasing affinity.

As shown in Scheme 1, 4-chloro-6,7-dimethoxyquinazoline (**2**) was used as a starting material<sup>29,30</sup> to synthesize according to described procedures<sup>19,29</sup> PD153035 (**3a**), anilines **3b–h**, *N*-methyl anilines **4a–c** and ethers **5a–d** analogs.

In Scheme 2, the corresponding ureas **6–7** were synthesized according to described procedures.<sup>19</sup>

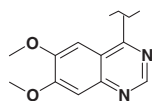
Selective reaction of the chloro derivative **2** with *meta*- or *para*-aminophenol in the presence of tetra-*n*-butylammonium bromide in a methyl ethyl ketone–sodium hydroxide mixture provided intermediates **8**<sup>29</sup> and **9**.<sup>19</sup> New carbamic acid esters **10–11** were obtained by amidification with corresponding amines. Compounds **8** and **9** reacted with corresponding isocyanates in chloroform to give the desired ureas **12**, **13a–b**,<sup>19</sup> **14a–b**,<sup>19</sup> **15–22** in high yields and after short reaction times (Scheme 3).

Inhibitory activity of the synthesised compounds against EGFR and VEGFR-2 tyrosine kinases was determined by measuring the levels of phosphorylation of the tyrosine-specific peptides (poly (Glu4-Tyr)substrate) in vitro. They were evaluated also for their antiproliferative activity towards the human endothelial-like, immortalized cell line EAhy926: this cell line is derived from the fusion of human umbilical vein endothelial (HUVEC) cells with the A549 human lung epithelial carcinoma cell line. These cells were used because of their role in angiogenesis. The cytotoxicities of the synthesised compounds were evaluated toward the hormone-independent PC3 prostate cancer cells, MCF7 breast cancer cells and HT29 colon cancer cells, by MTS test.

The kinase and cell data are summarized in Table 1. The first SAR study focused on the quinazoline skeleton substituted at the 4-position by aniline, *N*-methylaniline or an aryloxy group substituted by halides, amide, carbamate or urea. *N*-Methyl analogs, in particular **4a**, exhibited a good antiproliferative activity despite a complete absence of EGF- and VEGFR TK inhibitory effect. Recently we reported that the methylation of the aniline nitrogen of quinazolin derivatives is essential to obtain a drug binds to DNA as a typical intercalating agent.<sup>19</sup> Among the amide analogs **3d** and **5d**, no kinase inhibition and no antiproliferative effect was observed at 10  $\mu\text{M}$  concentration. Substitution by halogens showed some dual EGFR/VEGFR-2 kinase inhibition (**3a–c** and **5a–c**) with  $\text{IC}_{50}$  values <10  $\mu\text{M}$ . NH analogs **3a** and **3b** proved to be moderately potent EGFR inhibitors ( $\text{IC}_{50}$  values of 0.3 and 0.4  $\mu\text{M}$ , respectively) and compared favourably with their aryloxy counterparts (**5a** and **5b**). Introduction of donor–acceptor group such as carbamate or urea is generally more tolerated. The carbamic acid methyl ester **3e–f** showed no significant inhibition of EGFR (>5  $\mu\text{M}$ ) and VEGFR-2 (>5  $\mu\text{M}$ ). Replacing NH (**3e** and **3f**) with oxygen at the 4-position (**10** and **11**) exhibited good levels of inhibition against VEGFR-2 (0.7 and 0.6  $\mu\text{M}$ , respectively) but showed a significant decrease in activity against EGFR ( $\text{IC}_{50}$  >10  $\mu\text{M}$ ). All the urea-substituted aryloxy-quinazolines (**13a–b**, **14a–b**) were selectively active against VEGFR-2 with  $\text{IC}_{50}$  values <1  $\mu\text{M}$ . Compounds with *para*-substitution of urea on the aryl **13a**, **14a** (KDR  $\text{IC}_{50}$  = 0.07  $\mu\text{M}$ ) were 10-fold more efficient than their *meta*-analogs (**13b**, **14b**) and 100-fold more potent than the compounds with NH linker (**3g–h**). The strong inhibitory activity of these carbamates and ureas against VEGFR was not associated with antiproliferative activity (cell-based assays  $\text{IC}_{50}$  >10  $\mu\text{M}$ ).

A SAR study for the urea-substituted aryloxy-quinazolines **13–22** was undertaken. As shown in Table 2, *O*-linkage resulted in a selective inhibition of VEGFR-2. When urea was substituted by an alkyl group **12**, **22** (butyl and cyclohexyl), high potency for both VEGFR-2 was achieved ( $\text{IC}_{50}$  <1  $\mu\text{M}$ ). Diaryl ureas derivatives (**15–19**) resulted in excellent kinase inhibition with nanomolar  $\text{IC}_{50}$  value against KDR. Replacement of hydrogen with a halogen atom on the phenyl ring (**15–17**) was reasonably well tolerated. Bi-sub-

**Table 1**  
Enzymatic (EGFR/VEGFR-2) and cellular results for 6,7-dimethoxyquinazoline derivatives<sup>32</sup>



Compd	Enzymatic inhibitory (IC <sub>50</sub> , μM) <sup>a</sup>		% Proliferative inhibitory (or IC <sub>50</sub> , μM) <sup>d</sup>					
	EGFR <sup>b</sup>	VEGFR-2 <sup>c</sup>	Human prostate PC3	Human colorectal HT29	Human breast MCF-7	Human endothelial-like immortalized EAhy926		
Iressa <sup>®</sup>	0.07	14.80	7.40	ND	30%	ND		
Vandetanib	0.80	0.10	33%	4.20	26%	5.10		
R	X							
	NH	PD153035	0.063	ND	40%	10.10	4.70	7.10
	N-CH <sub>3</sub>	<b>4a</b> <sup>19</sup>	>10	>10	42%	6.10	9.20	3.95
	O	<b>5a</b>	7.60	9.80	27%	6%	0%	0%
	NH	<b>3b</b> <sup>31</sup>	0.38	5.30	6.50	5.70	4.90	4.50
	N-CH <sub>3</sub>	<b>4b</b>	>10	>10	22%	5.20	0%	46%
	O	<b>5b</b>	>10	9.50	5%	4.07	0%	ND
	NH	<b>3c</b>	5.70	1.65	1%	0%	31%	0%
	N-CH <sub>3</sub>	<b>4c</b>	>10	>10	15%	14%	0%	0%
	O	<b>5c</b>	5.90	0.60	16%	0%	0%	0%
	NH	<b>3d</b>	>10	>10	2%	0%	12%	0%
	O	<b>5d</b>	>10	>10	0%	0%	5%	3%
	NH	<b>3e</b>	6.90	5.80	2%	10%	27%	0%
	O	<b>10</b>	>10	0.70	0%	1%	4%	6%
	NH	<b>3f</b>	>10	5.60	12%	16%	6%	0%
	O	<b>11</b>	>10	0.60	28%	0%	0%	0%
	NH	<b>3g</b>	>10	5.10	35%	5.80	1.50	8.01
	N-CH <sub>3</sub>	<b>6a</b>	>10	>10	ND	ND	9.45	6.80
	O	<b>13a</b>	>10	0.06	23%	12%	12%	15%
	NH	<b>3h</b>	>10	6.20	43%	45%	7.15	36%
	N-CH <sub>3</sub>	<b>7a</b>	>10	>10	ND	ND	15%	27%
	O	<b>14a</b>	>10	0.07	12%	9%	0%	24%
	N-CH <sub>3</sub>	<b>6b</b>	>10	>10	0%	0%	0%	0%
	O	<b>13b</b>	>10	0.60	19%	7%	0%	12%
	N-CH <sub>3</sub>	<b>7b</b>	>10	>10	0%	0%	0%	0%
	O	<b>14b</b>	>10	0.60	19%	2%	0%	0%

ND: Not determined.

<sup>a</sup> Compounds tested at a concentration of 10 μM. Values correspond to  $n = 3$  (SD <10%).

<sup>b</sup> Inhibition of EGFR (purified from human carcinoma A431 cells) tyrosine kinase activity.

<sup>c</sup> Inhibition of VEGFR-2 (recombinant human protein) tyrosine kinase activity.

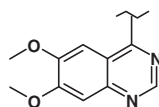
<sup>d</sup> Cell proliferation was measured by MTS assay at 10 μM (at least three independent experiments).

stitution at the 3- and 4-position by fluorine and chlorine on the phenyl ring (**17**) led to an excellent inhibitory activity against VEGFR-2. *ortho*-position of halide such as in compound **16** resulted in a weak decrease of activity against VEGFR-2. However, introduction of a bulkier naphthalene group (**20–21**) was envisaged and tolerated only with 2-naphthyl substituent (**20**): an unfavorable steric hindrance was observed with 1-naphthyl (**21**) resulting in IC<sub>50</sub> value of 5.50 μM. Its isomer position **20** was selectively active against VEGFR-2 with IC<sub>50</sub> value of 0.03 μM. These quinazolines were fur-

ther evaluated in cell-based assays but were inactive towards different cancer cell lines.

Table 3 shows the effects of variations of the linker on the central phenyl ring of compound **17**. Replacement of oxygen with a nitrogen atom (**23** and **24**)<sup>33</sup> led to a dramatically reduced enzymatic inhibition. The *O*-linkage therefore appears essential in order to obtain a VEGFR-2 selective inhibitor. To understand the observed difference, we explored the binding mode of these aryloxy quinazolines with KDR.

**Table 2**  
Enzymatic (EGFR/VEGFR-2) and cellular results for aryloxy-quinazolines derivatives **12–22**



Compd	Enzymatic inhibitory (IC <sub>50</sub> , μM) <sup>a</sup>		% Proliferative inhibitory (or IC <sub>50</sub> , μM) <sup>d</sup>				
	EGFR <sup>b</sup>	VEGFR-2 <sup>c</sup>	Human prostate PC3	Human colorectal HT29	Human breast MCF-7	Human endothelial-like immortalized EAhy926	
Iressa® Vandetanib	0.07 0.80	14.80 0.10	7.40 33%	ND 4.20	30% 26%	ND 5.10	
R	X						
<b>13a</b>		>10	0.06	23%	12%	12%	15%
<b>14a</b>		>10	0.07	12%	9%	0%	24%
<b>12</b>		>10	0.40	30%	8%	10%	0%
<b>15</b>		>10	0.05	2%	13%	10%	0%
<b>16</b>		>10	0.09	35%	10%	6.40	5.10
<b>17</b>		>10	0.04	36%	26%	30%	9.00
<b>18</b>		>10	0.06	40%	7.70	9.80	5.00
<b>19</b>		>10	0.05	23%	17%	23%	42%
<b>20</b>		>10	0.03	5%	0%	6.80	0%
<b>21</b>		>10	5.50	8%	17%	8%	9%
<b>22</b> <sup>28</sup>		>10	1.00	42%	8%	0%	31%

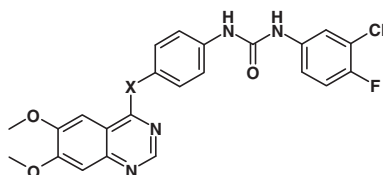
ND: Not determined.

<sup>a</sup> Compounds tested at a concentration of 10 μM. Values correspond to n = 3 (SD <10%).

<sup>b</sup> Inhibition of EGFR (purified from human carcinoma A431 cells) tyrosine kinase activity.

<sup>c</sup> Inhibition of VEGFR-2 (recombinant human protein) tyrosine kinase activity.

<sup>d</sup> Cell proliferation was measured by MTS assay at 10 μM (at least three independent experiments).

**Table 3**Biological activities of *N*-(3-chloro-4-fluorophenyl)-*N'*-[4-[6,7-dimethoxyquinazolin-4-yloxy]phenyl]urea **17** and the anilino analogs **23–24**

Compd	X	Enzymatic inhibitory (IC <sub>50</sub> , μM) <sup>a</sup>		% Proliferative inhibitory (or IC <sub>50</sub> , μM) <sup>d</sup>			
		EGFR <sup>b</sup>	VEGFR-2 <sup>c</sup>	Human prostate PC3	Human Colorectal HT29	Human breast MCF-7	Human endothelial-like immortalized EAhy926
<b>23</b>	NH	>10	4.30	9.40	6.20	7.70	5.30
<b>24</b>	N-CH <sub>3</sub>	>10	>10	ND	ND	35%	29%
<b>17</b>	O	>10	0.04	36%	26%	30%	9.00

ND: Not determined.

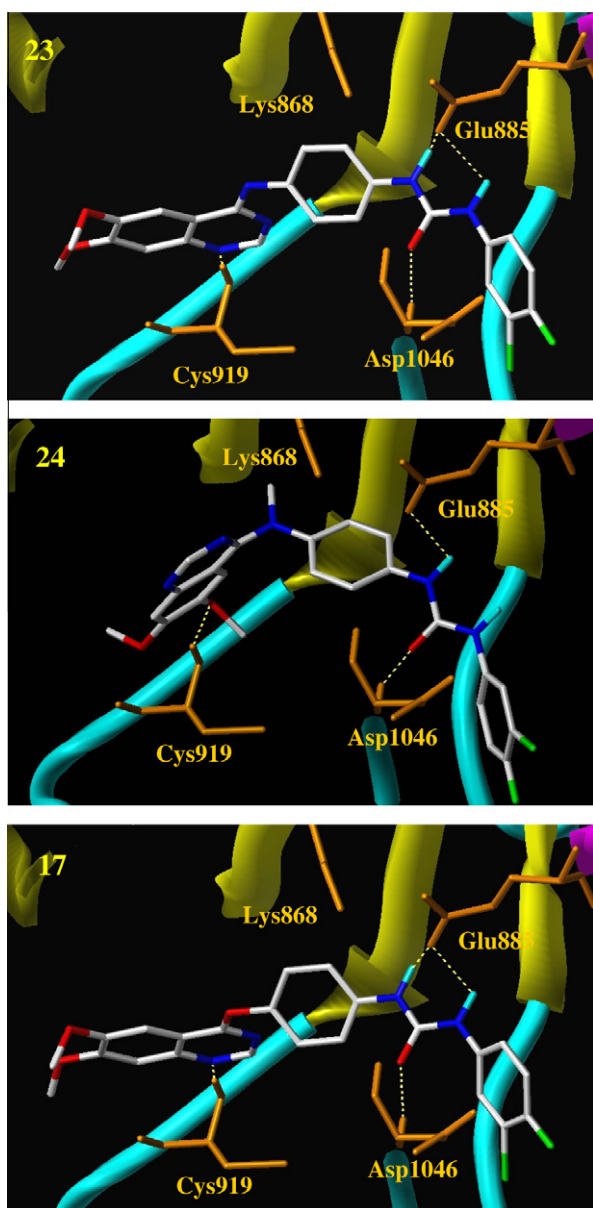
<sup>a</sup> Compounds tested at a concentration of 10 μM. Values correspond to *n* = 3 (SD <10%).<sup>b</sup> Inhibition of EGFR (purified from human carcinoma A431 cells) tyrosine kinase activity.<sup>c</sup> Inhibition of VEGFR-2 (recombinant human protein) tyrosine kinase activity.<sup>d</sup> Cell proliferation was measured by MTS assay at 10 μM (at least three independent experiments).**Figure 3.** Docking mode of compound **17** and its anilino analogs **23–24** at the ATP-site of VEGFR-2.

Figure 3 shows models of **17**, **23** and **24** bound to VEGFR-2, generated by molecular modeling.<sup>34</sup> As these models suggest, the anilino-urea **23** bound to the ATP-site of KDR in the same manner as its ether analog **17**. Particularly, the quinazoline cores adopt essentially volumes and conformations with identical orientations. We observed interactions between the CO and NH carbamate group with the backbone of Asp1046 and the Lys868–Glu885 salt bridge, respectively. H-bond interaction with Cys919 (between a cystein NH and the N1 nitrogen of quinazoline) was established. However, substitution by aniline at the 4-position of quinazoline (**23**) led to a displacement of the phenyl ring containing the urea group into the active site of VEGFR-2. This position would have a negative impact on the inhibition potency and limit donor-acceptor interaction of the urea moiety. In contrast, the NMe analog **24** adopts volumes and conformations in opposite directions compared to **17** and **23**. The phenyl ring of **24** is approximately perpendicular to the plane of the quinazoline core and this structure is expected to limit interaction with the active-site of VEGFR-2. This prediction is in line with the weaker activity observed for the quinazoline sub-series. We also briefly investigated the replacement of the terminal aromatic urea residue with an aliphatic group (data not shown) but this substitution further limited donor-acceptor interaction of urea, resulting in lower enzymatic activity of these derivatives. Consistent with the SARs in other series of urea class VEGFR-2 inhibitors, a diaryl urea moiety is favorable for optimal interaction with the hydrophobic back pocket of KDR kinase.

In summary, we have described the discovery, SAR studies and preliminary biological evaluation of a novel series of a VEGFR-2 selective tyrosine kinase inhibitor. We have investigated the replacement of linkers at the 4-position of a quinazoline skeleton by aryloxy, aniline and *N*-methylaniline entities. The diaryl urea of aryloxy-quinazoline potently inhibited VEGFR-2 at nanomolar concentrations. However their activity against VEGFR-2 is not associated with their antiproliferative activity on cell-based assays. Molecular modeling established the interactions of these compounds with the active binding site. Further modifications may be undertaken on the two phenyl groups of the urea moiety, and varying the methoxy groups on the quinazoline core may result in a better affinity and good antiproliferative activities.

#### Acknowledgments

The authors are grateful to the 'Ligue Nationale Contre le Cancer' (Comity of Pas-de-Calais-France) for its financial support.

We are grateful to Michael Howsam for critical comments on the manuscript.

## References and notes

- Levitzki, A. *Acc. Chem. Res.* **2003**, *36*, 462.
- Cohen, P. *Nat. Rev. Drug Disc.* **2002**, *1*, 309.
- Cohen, P. *Eur. J. Biochem.* **2001**, *268*, 5001.
- Zwick, E.; Bange, J.; Ullrich, A. *Trends Mol. Med.* **2002**, *8*, 17.
- Traxler, P.; Bold, G.; Buchdunger, E.; Caravatti, G.; Furet, P.; Manley, P.; O'Reilly, T.; Wood, J.; Zimmermann, J. *Med. Res. Rev.* **2001**, *21*, 499.
- Lohela, M.; Bry, M.; Tammela, T.; Alitalo, K. *Curr. Opin. Cell Biol.* **2009**, *21*, 154–165.
- Rahimi, N. *Exp. Eye Res.* **2006**, *83*, 1005.
- Roskoski, R., Jr. *Biochem. Biophys. Res. Commun.* **2004**, *319*, 1.
- Carmeliet, P. *Nat. Med.* **2003**, *9*, 653.
- Pandya, N. M.; Dhalla, N. S.; Santani, D. D. *Vasc. Pharmacol.* **2006**, *44*, 265.
- Otrock, Z. K.; Mahfouz, R. A. R.; Makarem, J. A.; Shamseddine, A. I. *Blood Cell Mol. Dis.* **2007**, *39*, 212.
- Roskoski, R., Jr. *Biochem. Biophys. Res. Commun.* **2008**, *375*, 287.
- Roskoski, R., Jr. *Crit. Rev. Oncol. Hematol.* **2007**, *62*, 179.
- Fayette, J.; Soria, J. C.; Armand, J. P. *Eur. Cancer Res.* **2005**, *41*, 1109.
- Sun, S.; Schiller, J. H. *Crit. Rev. Oncol. Hematol.* **2007**, *62*, 93.
- Denny, W. A. *Il Farmaco* **2001**, *56*, 51.
- Fry, D. W. *Exp. Cell Res.* **2003**, *284*, 131.
- Bridges, A. J.; Zhou, H.; Cody, D.; Rewcastle, G. W.; Mc-Michael, A.; Showalter, H. D.; Fry, D. W.; Kraker, A. J.; Denny, W. A. *J. Med. Chem.* **1996**, *39*, 267.
- Garofalo, A.; Goossens, L.; Baldeyrou, B.; Lemoine, A.; Ravez, S.; Six, P.; David-Coordonnier, M. H.; Bonte, J. P.; Depreux, P.; Lansiaux, A.; Goossens, J. F. *J. Med. Chem.* **2010**, *53*, 8089.
- Ranson, M.; Wardell, S. J. *Clin. Pharm. Ther.* **2004**, *29*, 95.
- Shepherd, F. A.; Rodrigues Pereira, J.; Ciuleanu, T.; Tan, E. H.; Hirsh, V.; Thongprasert, S.; Campos, D.; Maoleekoonpiroj, S.; Smylie, M.; Martins, R.; van Kooten, M.; Dediu, M.; Findlay, B.; Tu, D.; Johnston, D.; Bezjak, A.; Clark, G.; Santabarbara, P.; Seymour, L. *N. Eng. J. Med.* **2005**, *353*, 123.
- Nelson, M. H.; Dolder, C. R. *Ann. Pharmacother.* **2006**, *40*, 261.
- Ciardello, F.; Bianco, R.; Caputo, R.; Damiano, V.; Troiani, T.; Melisi, D.; De Vita, F.; De Placido, S.; Bianco, A. R.; Tortora, G. *Clin. Cancer Res.* **2004**, *10*, 784.
- Escudier, B.; Eisen, T.; Stadler, W. M.; Szczylik, C.; Oudard, S.; Siebels, M.; Negrier, S.; Chevreau, C.; Solska, E.; Desai, A. A.; Rolland, F.; Demkow, T.; Hutson, T. E.; Gore, M.; Freeman, S.; Schwartz, B.; Shan, M.; Simantov, R.; Bukowski, R. M. *N. Eng. J. Med.* **2009**, *49*, 332.
- Garofalo, A.; Goossens, L.; Lemoine, A.; Farce, A.; Arlot, Y.; Depreux, P. *J. Enzyme Inhib. Med. Chem.* **2010**, *25*, 158.
- Dent, P.; Curiel, D. T.; Fisher, P. B.; Grant, S. *Drug Resist. Update* **2009**, *12*, 65.
- Wedge, S. R.; Kendrew, J.; Hennequin, L. F.; Valentine, P. J.; Barry, S. T.; Brave, S. R.; Smith, N. R.; James, N. H.; Dukes, M.; Curwen, J. O.; Chester, R.; Jackson, J. A.; Boffey, S. J.; Kilburn, L. L.; Barnett, S.; Richmond, G. H.; Wadsworth, P. F.; Walker, M.; Bigley, A. L.; Taylor, S. T.; Cooper, L.; Beck, S.; Jürgensmeier, J. M.; Ogilvie, D. J. *Cancer Res.* **2005**, *15*, 389.
- Garofalo, A.; Goossens, L.; Lemoine, A.; Ravez, S.; Six, P.; Howsam, M.; Farce, A.; Depreux, P. *MedChemComm* **2011**, *2*, 65.
- Furuta, T.; Sakai, T.; Senga, T.; Osawa, T.; Kubo, K.; Shimizu, T.; Suzuki, R.; Yoshino, T.; Endo, M.; Miwa, A. *J. Med. Chem.* **2006**, *49*, 2186.
- Garofalo, A.; Goossens, L.; Lebegue, N.; Depreux, P. *Synthetic Commun.*, in press.
- Gibson, K. H.; Grundy, W.; Godfrey, A.; Woodburn, J. R.; Ashton, S. E.; Curry, B. J.; Scarlett, L.; Barker, A. J.; Brown, D. S. *Bioorg. Med. Chem. Lett.* **1997**, *7*, 2723.
- Cell culture and cell proliferation assays*: Human prostate cancer cells PC3 and breast cancer cell line MCF7 were grown at 37 °C in a humidified atmosphere containing 5% CO<sub>2</sub>, respectively in RPMI-1640 medium (Sigma) and MEM (Sigma) supplemented with 10% fetal bovine serum, glutamine (2 mM), penicillin (100 IU/mL), and streptomycin (100 µg/mL). HT29 colon cancer cell and EAhy926, umbilical cell immortalized, were grown at 37 °C in a humidified atmosphere containing 5% CO<sub>2</sub> in DMEM + Glutamax-1 (Gibco) supplemented with 10% fetal bovine serum, penicillin (100 IU/mL), and streptomycin (100 µg/mL).
- In the cell proliferation assay, cells were plated in triplicate on 96-well plates (3000 cells per well) and incubated for 24 h. Cells were then incubated in culture medium that contained various concentrations of tested compounds, each dissolved in less than 0.1% DMSO. After 72 h, cell growth was estimated by the colorimetric MTS test.
- In vitro kinase assays*: Kinase assays were performed in 96-well plates (Multiscreen Durapore, Millipore) using [ $\gamma$ -<sup>32</sup>P]ATP (Amersham Biosciences) and the synthetic polymer poly(Glu4/Tyr) (Sigma Chemicals) as a phospho-acceptor substrate. Tested compounds were dissolved in DMSO, final concentration of DMSO in assay solutions was 0.1%, which was shown to have no effect on kinase activity.
- EGFR tyrosine kinase activity*: 20 ng of EGFR (purified from human carcinoma A431 cells, Sigma Chemicals) were incubated for 1 h at 28 °C using various concentrations of tested compounds in kinase buffer (HEPES 50 mM pH 7.5, BSA 0.1 mg/mL, MnCl<sub>2</sub> 10 mM, MgCl<sub>2</sub> 5 mM, Na<sub>3</sub>VO<sub>4</sub> 100 µM, DTT 0.5 mM, poly(Glu4/Tyr) 250 µg/mL, ATP 5 µM, [ $\gamma$ -<sup>32</sup>P]ATP 0.5 µCi).
- VEGFR-2 tyrosine kinase activity*: 10 ng of VEGFR-2 (Recombinant Human Protein, Invitrogen) were incubated for 1 h at 28 °C using various concentrations of tested compounds in kinase buffer (Tris 50 mM pH 7.5, BSA 25 µg/mL, MnCl<sub>2</sub> 1.5 mM, MgCl<sub>2</sub> 10 mM, DTT 2.5 mM, Na<sub>3</sub>VO<sub>4</sub> 100 µM,  $\beta$ -glycerophosphate 5 mM, poly(Glu4/Tyr) 250 µg/mL, ATP 5 µM, [ $\gamma$ -<sup>32</sup>P]ATP 0.5 µCi).
- The reaction was stopped by adding 20 µL of trichloroacetic acid 100%. Wells were screened out and washed 10 times with trichloroacetic acid 10%. Plates were counted in a Top Count for 1 min per well.
- Melting points were determined in open capillary tubes on a Büchi reference B-530 digital melting point apparatus and are uncorrected. Kieselgel 60 F-254 commercial plates were used for analytical TLC as well as UV light with/without iodine to follow the course of the reaction. Silica gel Kieselgel Si 60, 0.063–0.200 mm (Merck) was used for column chromatography. The structures of all compounds were determined by IR (using a Bruker VECTOR 22 instrument) <sup>1</sup>H NMR (300 MHz) spectra were recorded on a Bruker AC300P NMR spectrometer in DMSO-*d*<sub>6</sub> or in CDCl<sub>3</sub> at room temperature. APCI+ (Atmospheric Pressure Chemical Ionization) mass spectra were obtained on an LC-MS system Thermo Electron Surveyor MSQ.
- Compound 17**: <sup>1</sup>H NMR (DMSO)  $\delta$ <sub>H</sub> 3.95 (s, 3H), 3.97 (s, 3H), 7.20–7.40 (m, 3H), 7.50–7.70 (m, 6H), 8.52 (s, 1H), 8.90 (s, 1H), 8.92 (s, 1H). LC-MS (APCI+): *m/z* 469 (MH<sup>+</sup>) and 471 (M+2+H<sup>+</sup>)—tr (min): 4.02.
- Compound 23**: <sup>1</sup>H NMR (DMSO)  $\delta$ <sub>H</sub> 3.95 (s, 3H), 3.97 (s, 3H), 7.02 (m, 1H), 7.19 (s, 1H), 7.31 (m, 1H), 7.48 (d, 2H, *J* = 9.00 Hz), 7.62 (d, 2H, *J* = 9.00 Hz), 7.95 (s, 1H), 8.08 (m, 1H), 8.54 (s, 1H), 8.58 (s, 1H), 9.21 (s, 1H), 10.11 (s, 1H). LC-MS (APCI+): *m/z* 468 (MH<sup>+</sup>) and 470 (M+2+H<sup>+</sup>)—tr (min): 3.11.
- Compound 24**: <sup>1</sup>H NMR (DMSO)  $\delta$ <sub>H</sub> 3.61 (s, 3H), 3.88 (s, 3H), 3.95 (s, 3H), 6.58 (d, 1H, *H*<sub>o</sub> = 7.40 Hz), 6.98 (d, 2H, *J* = 8.40 Hz), 7.05–7.15 (m, 2H), 7.20 (d, 2H, *J* = 8.40 Hz), 7.64 (s, 1H), 7.79 (d, 1H, *J* = 4.40 Hz), 7.91 (s, 1H), 8.61 (s, 1H), 8.87 (s, 1H). LC-MS (APCI+): *m/z* 482 (MH<sup>+</sup>) and 484 (M+2+H<sup>+</sup>)—tr (min): 3.43.
- Molecular modeling**: All the calculations have been carried out under the Sybyl 6.9.1 molecular modeling package running on Silicon Graphics Octane 2 workstations. The ligands were built from the internal fragments library of Sybyl and their geometry was optimized by the Powell method available in the Maximin2 procedure to a gradient of 0.001 Kcal/mol Å. The dielectric constant was set to 4 to implicitly represent a biological medium the atomic charges were attributed following the Gasteiger–Hückel method and the energy minimization was run with the Tripos force field. The structure of the protein co-crystallized with an inhibitor was obtained from the Protein Data Bank (<http://www.pdb.org>) under the entry 1YWN.